

Gabor deconvolution

Gary F. Margrave and Michael P. Lamoureux

ABSTRACT

The Gabor transform decomposes a 1-D temporal signal onto a time-frequency plane. Temporal localization is accomplished by windowing the signal with a Gaussian *analysis window* translated to any particular time. The Fourier transform of the windowed signal provides frequency information for the time of the window centre. The inverse Gabor transform is an integration over the time-frequency plane using an optional *synthesis window*. The discrete Gabor transform has an approximate realization based on the fact that a shifted suite of Gaussians can sum to unity. Gabor filters are nonstationary filters that can be implemented by multiplying the Gabor transform of a signal by a time-frequency filter specification. Extreme cases of Gabor filters are shown to correspond to normal or adjoint pseudodifferential operators. Gabor deconvolution is developed for exploration seismology based on a nonstationary convolutional model of a seismic trace. This model predicts that the Gabor transform of a seismic signal decomposes as the Fourier spectrum of the source signature times the symbol of a forward Q-filter times the Gabor transform of the reflectivity. Gabor deconvolution requires the spectral factorization of the Gabor transform of the seismic signal into a reflectivity part times a propagating wavelet part. This factorization can be done on magnitude spectra with phase being determined from a minimum-phase condition. Testing on synthetic data shows the nonstationary Gabor deconvolution is an effective tool that combines the processes of stationary deconvolution, inverse Q-filtering, and gain adjustment.

INTRODUCTION

The deconvolution of seismic data is a fundamental part of the construction of high-resolution seismic images. Deconvolution addresses the challenging task of separating a seismic trace (i.e. the recording of a single sensor) into two components, both unknown, representing the seismic waveform and the reflectivity (the latter is a time series of reflection coefficients). That this can be done at all is remarkable and the first solutions were the achievement of the mathematician Norbert Wiener and his students though the application was radar not seismology. Enders Robinson and Sven Treitel (1967) were pioneers in bringing the technique to geophysics.

This separation of a seismic trace into two parts exploits reasonable assumptions about the nature of the seismic waveform and reflectivity and another assumption about the seismic trace itself. The seismic waveform is postulated to be a temporally short pulse, implying a smooth Fourier transform, the amplitude and phase spectra of which are linked by the minimum-phase condition. The latter is a consequence of linearity and causality and says that the phase spectrum can be calculated as the Hilbert transform of the logarithm of the amplitude spectrum (e.g. Claerbout, 1976 and other basic texts). The reflectivity is postulated to be a random time-series whose autocorrelation therefore is nonzero only at zero lag and whose power spectrum is a constant at all frequencies.

The final assumption is that the seismic signal is assumed to have the property of stationarity. Though intuitively rather obvious, stationarity is difficult to define in a truly useful way. A common definition requires that the seismic trace, $s(t)$, be regarded as one *realization* of a random process. If many other realizations of the same random process are available (perhaps from geophones placed in parallel quantum universes) then the *expectation value* at any time is defined as the average taken over the entire, possibly infinite, ensemble of realizations at that time. If this expectation value is found to be independent of time, then the signal is said to be stationary. Of course, such ensembles are not often encountered in practice so an alternative test for stationarity is useful. Commonly, the ensemble average is replaced by a time average of the signal multiplied by some localizing window. (Signals with the property that ensemble averages and time averages are equal are called *ergodic*.) Practically then, a signal is stationary if such time averages are independent of time. Among the many drawbacks of this definition is the fact that it depends upon the localizing window. A signal may be stationary with respect to one window and nonstationary with respect to another.

A more common test of stationarity is to require that the power spectrum of the localized signal is independent of the time of localization. This is also a difficult criterion to apply because real signals are finite in length and, if such a signal is stationary by the ensemble average test, it will generally still show variations in local power spectra. Therefore, some level of power fluctuation is generally tolerated in signals that are called stationary.

The difficulty of employing these definitions without ambiguity in a practical setting motivates us to avoid them as far as is possible. When confronted with an unknown signal we resist the temptation to term it stationary or nonstationary on the basis of statistical measures. Instead, we prefer to employ external information such as a physical model to make this distinction. For example, in the seismic deconvolution case we argue that seismic waves always suffer irreversible, frequency-dependent energy loss as they propagate and are therefore necessarily nonstationary. Thus we shift attention from the signals to the generating processes.

In mathematical terms, if we can model a signal as a nonstationary filter applied to a stationary input, then we say it is nonstationary. The prototypical nonstationary filter is a pseudodifferential operator. Therefore, if the signal is expressible as a pseudodifferential operator applied to a stationary signal, then it is nonstationary. The input might be called stationary because it is generated by a stationary process. We will present such a nonstationary seismic trace model and use it as the basis for our deconvolution procedure.

The fundamental goal of our paper is to develop an extension of seismic deconvolution to the nonstationary setting. For this purpose we outline and employ the Gabor transform. First the continuous Gabor transform is discussed and then the discrete theory is approached. We develop a novel discrete Gabor transform that, while approximate, has an easily controlled error term and a simple numerical implementation. Then we present a class of Gabor filters and explore their relation to pseudodifferential operators. After this introductory material, we develop a nonstationary mathematical model for a seismic trace and argue its validity on

physical grounds. We then derive an expression for the Gabor transform of this trace model. This expression guides our Gabor deconvolution algorithm. We argue that the Gabor transform of a seismic signal can be processed in such a way that the contribution from reflectivity is suppressed to produce an estimate of the *propagating wavelet*. When the unaltered Gabor transform of the signal is divided by the estimate of the propagating wavelet, the result estimates the Gabor transform of the reflectivity. We close our paper with a numerical example.

THE GABOR TRANSFORM

In 1946, Dennis Gabor, the inventor of the hologram, published a paper in which he proposed the expansion of a wave in terms of *Gaussian wave packets*. An example of such a wave packet is a sine wave multiplied by a Gaussian function. The theory of the Fourier transform assures that a complete set (all possible frequencies) of sine waves will allow an arbitrary function to be represented. When multiplied by a Gaussian, these sine waves become *localized* but it is reasonable to expect that they can still form a local expansion basis. Thus, if a signal is modulated (multiplied) by a Gaussian window of a certain width and centred at time t_0 , then a Fourier expansion of the modulated signal gives a measure of the *local spectrum*. Clearly such a spectrum is not unique since the width of the Gaussian is arbitrary; but nevertheless, such local spectra are extremely useful. If a collection of local spectra is computed for a suite of window positions, the result is a *time-frequency decomposition* of the signal. Furthermore, if the signal can be reconstructed from this decomposition, then a nonstationary filter can be achieved by modifying the decomposition first. A time-frequency decomposition of a signal created in this manner is called a *Gabor transform*.

The Gabor transform can be developed for a continuous or discrete set of window positions. The continuous Gabor transform follows easily from the theory of the Fourier transform. The signal can obviously be reconstructed from its Gabor transform since it can be constructed from a single local Fourier spectrum by inverse Fourier transformation and demodulation. This makes it apparent that the Gabor transform is a highly redundant representation of a signal. Nevertheless, the inverse of the continuous Gabor transform is constructed from the entire Gabor spectrum by superposition of the local spectra after inverse Fourier transformation without demodulation.

The discrete Gabor transform is much more difficult to develop. The redundancy of the continuous Gabor transform suggests a discrete set of window positions should suffice; however, this was not proven until Bastiaans (1980). The theory of the discrete Gabor transform that has developed since then is, like the wavelet transform, built upon the concept of an *expansion frame*. Similar to an orthogonal basis, an expansion frame allows an arbitrary function to be written as a scalar-weighted superposition of elementary functions. However, while the scalar weights for the orthogonal basis are formed by the inner product of the orthogonal basis function with the signal, for the frame expansion the inner product is taken not against the frame expansion function but rather against the corresponding function from the *dual frame*. The calculation of this dual frame is a major technical challenge. For the Gabor expansion, the expansion frame may be the Gaussian-modulated complex

exponentials; although the theory generalizes to windows other than Gaussians. The dual frame that is required to compute the expansion coefficients is a complex exponential modulated by the dual window. A complete overview of the theory of the discrete Gabor transform is found in Feichtinger and Strohmer (1998).

In this paper, we present the theory of the continuous Gabor transform and only an approximate theory for the discrete transform. Our approximate discrete transform does not exactly recreate the original signal, but we show that the loss can be made as small as desired.

The continuous Gabor transform

Following Mertins (1999), we define the continuous Gabor transform (GT) of a signal $s(t)$ as

$$V_g s(\tau, f) = \int_{-\infty}^{\infty} s(t) g(t - \tau) e^{-2\pi i f t} dt \quad (1)$$

where $g(t)$ is the Gabor analysis window and τ is the location of the window centre. Although in the present work we generally use $g(t)$ to be a Gaussian function, we remark that this need not be the case and that the theory works well for quite general windows including Dirac delta distributions. Given $V_g s(\tau, f)$, the signal can be reconstructed from the expression

$$s(t) = \int_{-\infty}^{\infty} \int_{-\infty}^{\infty} V_g s(\tau, f) \gamma(t - \tau) e^{2\pi i f t} df d\tau \quad (2)$$

where $\gamma(t)$ is the Gabor synthesis window. The analysis and synthesis windows must satisfy the condition

$$\int_{-\infty}^{\infty} g(t) \gamma(t) dt = 1 \quad (3)$$

Proof: Substitute equation (1) into equation (2) to get

$$\int_{-\infty}^{\infty} \int_{-\infty}^{\infty} V_g s(\tau, f) \gamma(t - \tau) e^{2\pi i f t} df d\tau = \int_{-\infty}^{\infty} \int_{-\infty}^{\infty} \int_{-\infty}^{\infty} s(t') g(t' - \tau) e^{-2\pi i f t'} dt' \gamma(t - \tau) e^{2\pi i f t} df d\tau \quad (4)$$

Next we assume that the integrands are sufficiently well behaved to allow the order of integration to be exchanged and perform the f integral first. Since f dependence occurs only in the complex exponentials, this becomes

$$f \text{ integral} = \int e^{2\pi i [t-t'] f} df = \delta(t-t') \quad (5)$$

where $\delta(t-t')$ is the Dirac delta function. Thus equation (4) becomes

$$\int_{-\infty}^{\infty} \int_{-\infty}^{\infty} V_g s(\tau, f) \gamma(t-\tau) e^{2\pi i f t} df d\tau = \int_{-\infty}^{\infty} \int_{-\infty}^{\infty} s(t') g(t'-\tau) \gamma(t-\tau) \delta(t-t') dt' dt \quad (6)$$

Now consider the τ integral. Since τ dependence occurs only in the window functions, this integral becomes

$$\int_{-\infty}^{\infty} g(t'-\tau) \gamma(t-\tau) d\tau = \int_{-\infty}^{\infty} g(u) \gamma(t-t'+u) du = \Lambda(t-t') \quad (7)$$

where $\Lambda(t-t')$ simply symbolizes the result of the integration; but we note that, according to equation (3) $\Lambda(0)=1$. Thus we write equation (6) as

$$\int_{-\infty}^{\infty} \int_{-\infty}^{\infty} V_g s(\tau, f) \gamma(t-\tau) e^{2\pi i f t} df d\tau = \int_{-\infty}^{\infty} s(t') \Lambda(t-t') \delta(t-t') dt' = s(t). \quad (8)$$

The last step, that completes the proof, follows from the defining property of the Dirac delta function and the fact that $\Lambda(0)=1$.

In closing this section, we note several distinctive things about the Gabor transform pair. First, the forward transform maps a one-dimensional signal to a two-dimensional spectrum whose properties are determined by the nature of the signal and of the analysis window. Second, the inverse transform is a two-dimensional operation that collapses the spectrum into a one-dimensional signal. As with the Fourier transform, there is an integration over frequency; but additionally, there is an integration over window position. Finally, given an analysis window, the synthesis window is not uniquely determined. In particular, the windows $g \equiv 1$ or $\gamma \equiv 1$ are always possible provided that the nontrivial window is suitably normalized. The Gabor transform reduces to the Fourier transform if both the analysis and synthesis windows are unity.

An approximate discrete Gabor transform

The discrete Gabor transform (DGT) decomposes the signal on a time-frequency lattice whose spacings, say $\Delta\tau$ and Δf , are ideally as coarse as possible to minimize the redundancy of information. For the ordinary discrete Fourier transform (DFT), $\Delta f = (N\Delta t)^{-1}$ where N is the number of samples in the signal and Δt is the temporal sample interval. We can regard the DFT as an end member case of the DGT with a single window position and an analysis window $g \equiv 1$. In this case, $\Delta\tau = N\Delta t$, that is the spacing of the temporal window position is equal to the length of the signal. Then, for the DFT, $\Delta f \Delta\tau = (N\Delta t)^{-1} N\Delta t = 1$. If we now choose a smaller $\Delta\tau$, it would be

desirable to increase Δf such that $\Delta f \Delta \tau \approx 1$ so that the DGT is described by a similar number of lattice points as the DFT. This goal has proven elusive, although its pursuit has resulted in some very beautiful mathematics, much of which is found in Feichtinger and Strohmer (1998).

The Gabor frame

As a brief sketch, let the *Gabor frame* be given by

$$g_{m,n}(t) = g(t - m\Delta\tau) e^{-2\pi i m \Delta f} \quad (9)$$

then the DGT (also called the analysis mapping) is

$$(T_g s)_{m,n} = \int_{-\infty}^{\infty} s(t) g_{m,n}(t) dt \equiv \langle s, g_{m,n} \rangle. \quad (10)$$

If the Gabor frame of equation (9) were an orthonormal basis, then we would expect to recover the signal $s(t)$ from the Gabor frame operator S_g defined by

$$S_g s(t) = \sum_{m,n \in \mathbb{Z}} \langle s, g_{m,n} \rangle g_{m,n}(t). \quad (11)$$

For example, the DFT, using the orthonormal basis $h_n(t) = e^{2\pi i t n \Delta f}$, recovers a signal exactly from the expansion $s(t) = \sum_{n \in \mathbb{Z}} \langle s, h_n \rangle h_n(t)$. Since the $g_{m,n}$ form a frame and not an orthonormal basis, for the DGT, the recovery of the signal from equation (11) requires the inversion of the Gabor frame operator. That is

$$s(t) = \sum_{m,n \in \mathbb{Z}} \langle s, g_{m,n} \rangle S_g^{-1} g_{m,n}(t) = \sum_{m,n \in \mathbb{Z}} \langle s, g_{m,n} \rangle \gamma_{m,n}(t) \quad (12)$$

where $\gamma_{m,n}(t) = S_g^{-1} g_{m,n}(t)$ is called the *dual Gabor frame*. So, if the Gabor frame operator can be inverted then the inverse DGT (equation 12) can exactly recover the signal.

The Gabor frame is known to be complete in $L^2(\mathbb{R})$ if and only if $\Delta f \Delta \tau \leq 1$. (In the mathematical literature, it is customary to denote the lattice spacings by a and b and to write $ab \leq 1$.) This means that for $\Delta f \Delta \tau > 1$, the set $\{g_{m,n}\}$ fails the conditions required to be a frame (not given here). Furthermore, it is known that in the critical sampling case of $\Delta f \Delta \tau = 1$ there is no known numerically stable algorithm to invert the Gabor frame operator. For the oversampled cases $\Delta f \Delta \tau < 1$, the frame operator can be inverted but the closer it gets to critical sampling the greater the numerical problems.

An approximate discrete Gabor transform

Our approximation relies upon a special property of Gaussians that links the Gaussian width with the spacing between Gaussians $\Delta\tau$. That is, it is possible to choose a set of Gaussians such that

$$\sum_{k \in \mathbb{Z}} g(t - k\Delta\tau) \approx 1 \quad (13)$$

$$g(t - k\Delta\tau) = \frac{\Delta\tau}{T\sqrt{\pi}} e^{-[t - k\Delta\tau]^2 T^{-2}}$$

where

(14)

with T being the Gaussian (half) width. More precisely, in Appendix A, we show that

$$\sum_{k \in \mathbb{Z}} g(t - k\Delta\tau) = 1 + 2 \cos(2\pi t / \Delta\tau) e^{-[\pi T / \Delta\tau]^2} + \dots \quad (15)$$

Here the second term estimates the error (all remaining terms are exponentially smaller) in the approximation. Thus the error can be made arbitrarily small by increasing the ratio $T / \Delta\tau$. The maximum error is -21 decibels for $T / \Delta\tau = .5$, -85 decibels for $T / \Delta\tau = 1$, -150 decibels for $T / \Delta\tau = 1.5$ and -340 decibels $T / \Delta\tau = 2$. Thus for $T / \Delta\tau > 1.5$ the error is negligible for most geophysical purposes. Figure 1 illustrates a Gaussian sum for the case of $T = .1$ and $\Delta\tau = .05$ over the interval $0 \leq \tau \leq 1$. We note a very good approximation to unity except within about $2T$ of either end. Many other such *partitions of unity* are possible for various choices of $(T, \Delta\tau)$. Equation (14) shows that the more closely packed the Gaussians are, the smaller are their individual amplitudes. Figure 2 shows a suite of summation curves for $T = .1$ and $\Delta\tau = \{0.01, 0.025, 0.05, 0.1, 0.15, 0.2\}$. As $\Delta\tau / T$ significantly exceeds unity then the cosine error term in equation (15) becomes apparent.

Under the assumption that a set of Gaussian windows has been chosen that makes the sum in equation (13) as close to unity as desired, we decompose a seismic signal into Gaussian slices as

$$s(t) = s(t) \sum_{k \in \mathbb{Z}} g(t - k\Delta\tau) = \sum_{k \in \mathbb{Z}} s(t) g(t - k\Delta\tau) = \sum_{k \in \mathbb{Z}} s_k(t) \quad (16)$$

where the Gaussian slice is defined to be $s_k(t) = s(t) g(t - k\Delta\tau)$. Next we apply a forward Fourier transform

$$\hat{s}(f) = \sum_{k \in \mathbb{Z}} \int_{-\infty}^{\infty} s_k(t) e^{-2\pi i f t} dt = \sum_{k \in \mathbb{Z}} \hat{s}_k(f) \quad (17)$$

where \hat{s} is the Fourier transform of s and

$$\widehat{s}_k(f) \equiv \int_{-\infty}^{\infty} s_k(t) e^{-2\pi ift} dt \quad (18)$$

is our approximate Gabor transform. As written, it is discrete in the window position coordinate, as indexed by k , but continuous in frequency f . Of course, in a computer implementation, we would replace the integral Fourier transform with the DFT as

$$\hat{s}_m = \sum_{k \in \mathbb{Z}} \sum_{j \in \mathbb{Z}} s_{j,k} e^{-2\pi i m j / N} = \sum_{k \in \mathbb{Z}} \widehat{s}_{k,m} \quad (19)$$

where j runs over the time-domain samples of the discrete signal, $s_{j,k}$ is the k^{th} Gaussian slice, and the fully discrete Gabor transform is

$$\widehat{s}_{k,m} = \sum_{j \in \mathbb{Z}} s_{j,k} e^{-2\pi i m j / N} \quad . \quad (20)$$

We continue our discussion using the semi-discrete transform of equation (18), though the analogous formulae for the fully discrete case are easily deduced.

The recovery of the original signal from $\widehat{s}_k(f)$ follows by simply taking the inverse Fourier transform of equation (17)

$$s(t) = \int_{-\infty}^{\infty} \left[\sum_{k \in \mathbb{Z}} \widehat{s}_k(f) \right] e^{2\pi i f t} df \quad . \quad (21)$$

Thus $\widehat{s}_k(f)$ is simply summed over k and then inverse Fourier transformed. In comparison with the theory of the continuous Gabor transform given previously, we have presented a Gabor methodology that uses a special discrete set of analysis windows, such that equation (13) is satisfied, and uses a synthesis window of $\gamma \equiv 1$. We have avoided the difficult issue of inverting the Gabor frame operator by using a special set of windows and accepting an approximate transform. In the next section, in the context of Gabor filtering, we will introduce a non-trivial synthesis window.

As a test of this approximate Gabor transform, a seismic signal was forward and inverse Gabor transformed and is compared to the original signal in Figure 3. The difference plot shows that the most significant differences occur at the ends of the signal. This is due to the fact that the Gaussian summation of equation (13) must be conducted over a finite line segment and has significant departures from unity near the ends of the segment (Figure 1). The inherent error in the transform can be reduced by a simple normalization procedure in which the Gabor transform is divided by the summation curve. That is, let $h(t) = \sum_{k \in \mathbb{Z}} g(t - k \Delta \tau)$ be the actual summation curve employed in a Gabor transform. The Gabor transform of equation (18) can be normalized by

$$\widehat{s}_k(f) \equiv \frac{\int_{-\infty}^{\infty} s_k(t) e^{-2\pi ift} dt}{h(k\Delta\tau)}. \quad (18a)$$

Figure (4) is a recreation of the test of Figure (3) using the normalized transform of equation (18a). The end effects are clearly reduced, though not eliminated, by the normalization.

The Gabor transform of a signal is not unique and depends strongly on the Gaussian half-width T and the window increment $\Delta\tau$. Figure 5 shows eight versions of the Gabor transform of the nonstationary signal of Figures 3 and 4. The larger T is, the greater is the frequency resolution but at the expense of temporal resolution. As T decreases, frequency resolution is lost but temporal resolution increases. When temporal resolution is low, a small $\Delta\tau$ results in a highly redundant transform; conversely, when $\Delta\tau$ is large and temporal resolution is high, the transform can actually be undersampled in τ . This tradeoff in time-frequency resolution is often called the uncertainty principle and has been known since at least the early days of Quantum mechanics. The Gaussian window is unique in that, for a given window width, it is known to give the best possible simultaneous resolution in both time and frequency compared to all other possible windows.

GABOR FILTERING

A filter can be implemented using the Gabor transform by simply modifying the Gabor spectrum of a signal prior to the reconstruction. We describe the filter by its nonstationary transfer function, $\alpha(\tau, f)$, and illustrate its application to a signal $s(t)$ using the continuous Gabor transform as

$$s_\alpha(t) = \int_{-\infty}^{\infty} \int_{-\infty}^{\infty} \alpha(\tau, f) V_g s(\tau, f) \gamma(t - \tau) e^{2\pi ift} df d\tau. \quad (22)$$

We now examine two limiting forms of this general Gabor filter. First consider the case when $\gamma(t - \tau) \equiv 1$. In this case, we refer to a Gabor filter of type 1, or an *analysis window filter*, and write

$$s_{\alpha 1}(t) = \int_{-\infty}^{\infty} \int_{-\infty}^{\infty} \alpha(\tau, f) V_g s(\tau, f) e^{2\pi ift} df d\tau. \quad (23)$$

This filter is achieved by forming the product of the Gabor transform with the nonstationary transfer function, averaging over τ , and inverse Fourier transforming.

Second, consider the case when $\gamma(t - \tau) \equiv 1$ and note that in this case the Gabor transform reduces to the Fourier transform. We call this a Gabor filter of type 2, or a synthesis window filter, and it is given by

$$s_\alpha(t) = \int_{-\infty}^{\infty} \int_{-\infty}^{\infty} \alpha(\tau, f) \hat{s}(f) \gamma(t - \tau) e^{2\pi i f t} df d\tau . \quad (24)$$

This filter begins with the product of the Fourier transformed signal and the nonstationary transfer function, then applies an inverse Fourier transform, and finally applies the synthesis window and averages over τ . In the limit as $\gamma(t - \tau) \rightarrow \delta(t - \tau)$, equation (24) becomes a standard-form Kohn-Nirenberg pseudodifferential operator. Similarly, in the limit $g(t - \tau) \rightarrow \delta(t - \tau)$, equation (23) becomes an adjoint-form (or dual-form) Kohn-Nirenberg pseudodifferential operator. Thus, the general Gabor filter of equation (22) becomes a standard form Kohn-Nirenberg pseudodifferential operator if $g \equiv 1$ and $\gamma \equiv \delta$ while it reduces to an adjoint form if $g \equiv \delta$ and $\gamma \equiv 1$. In this sense, Gabor filters generalize pseudodifferential operators.

We now present formulae for the two limiting forms of Gabor filters based on our approximate semi-discrete Gabor transform. For this purpose, the nonstationary transfer function must be specified in a semi-discrete fashion as $\alpha_k(f)$. The analysis window filter is then

$$s_{\alpha 1}(t) = \int_{-\infty}^{\infty} \sum_{k \in \mathbb{Z}} \alpha_k(f) \widehat{s}_k(f) e^{2\pi i f t} df \quad (25)$$

while the synthesis window filter is

$$s_{\alpha 2}(t) = \sum_{k \in \mathbb{Z}} \gamma(t - k \Delta \tau) \int_{-\infty}^{\infty} \alpha_k(f) \hat{s}(f) e^{2\pi i f t} df . \quad (26)$$

For a given nonstationary transfer function, a form intermediate to these two filters can be obtained by the formula

$$s_{\alpha 3}(t) = \sum_{k \in \mathbb{Z}} \gamma(t - k \Delta \tau) \int_{-\infty}^{\infty} \sqrt{\alpha_k(f)} \sum_{m \in \mathbb{Z}} \sqrt{\alpha_m(f)} \widehat{s}_m(f) e^{2\pi i f t} df . \quad (27)$$

This splits the filter between the two extreme cases by applying the square root of the transfer function as an analysis filter and again, as a synthesis filter.

SEISMIC DECONVOLUTION WITH THE GABOR TRANSFORM

We have developed an approach to the seismic deconvolution using the Gabor transform that extends the stationary deconvolution theory of Wiener spiking deconvolution (e.g. Robinson and Treitel 1967) to the nonstationary case. The stationary theory is based on a simple convolutional model of a seismic trace that is often written

$$s(t) = (r \bullet w)(t) \equiv \int_{-\infty}^{\infty} w(t-\tau) r(\tau) d\tau \quad (28)$$

where $w(t)$ is the *seismic wavelet* and $r(t)$ is the *reflectivity*. The term reflectivity refers to a time series the samples of which are the normal incidence P-wave reflection coefficients of subsurface reflectors positioned at the normal incidence traveltimes to each reflector. This model is often justified on physical grounds using the Green's function approach to solving partial differential equations. It is argued that, if the *impulse response* (i.e. solution for a Dirac delta-function source $\delta(t)$) of the wave equation is known, then the solution for a temporally extended source is given by the convolution of the source waveform (wavelet) with the impulse response. However, this argument only implies equation (28) if $r(t)$ is interpreted to be the impulse response, a much more complex time series than the reflectivity. In addition to normal incidence reflection coefficients representing primary reflections, the impulse response also contains all possible multiply-scattered waves. The viewpoint that $r(t)$ is the impulse response and $w(t)$ is the source signature leads to gapped predictive deconvolution algorithms such as described in Peacock and Treitel (1969) that are intended to estimate and subtract the multiple sequence. In this case, the goal of deconvolution is not only to estimate and remove the source signature but also to somehow transform the impulse response into the simpler reflectivity. An alternative viewpoint is to argue that the multiples can be considered as part of the seismic wavelet so that $r(t)$ can still be reflectivity. Then the deconvolution technique seeks to estimate $r(t)$ by removing $w(t)$. Regardless of which perspective, impulse response or reflectivity, is taken, the goal of a deconvolution process is to estimate reflectivity not impulse response.

Either of these perspectives of equation (28) is hindered by the same complexity and that is the fundamental nonstationarity of the seismic response. On one level, nonstationarity refers to the fact that the earth is not a perfectly elastic medium and that seismic waves lose energy to molecular heat as they propagate. The simplest model of this absorption is the constant-Q model of Kjartansson (1979). (Constant Q refers to a Q that is independent of frequency but may depend upon space or traveltime.) Since this loss is a function of the ratio of wavelength to propagation distance, the seismic wavelet progressively evolves as it illuminates each reflector. Futterman (1962) proved that in a dissipative medium that is both linear and causal then the wavelet evolves according to what is now called a minimum-phase condition. This means, that at any instant of time, the phase spectrum of the wavelet is the Hilbert transform of the natural logarithm of the amplitude spectrum.

On another level, even if the medium is not dissipative the effective seismic wavelet still evolves as it propagates. This is due to the effect of many local interbed multiples that build up the *tail* of the wavelet as was first explained by O'Doherty and Anstey (1971). Called stratigraphic filtering, the effect of these multiples is to attenuate high frequencies in a manner similar to dissipation though the applicability of the minimum-phase condition is in doubt. In practice, it is essentially impossible to separate the effects of stratigraphic filtering from those of dissipation. Instead, a single effective Q is estimated that is assumed to roughly account for both effects.

If the impulse response of a linear, dissipative wave equation is known, then equation (28) still suffices to apply the source waveform because the Green's function method is still valid. However, a deconvolution that removes the source waveform, thereby estimating the nonstationary impulse response, has accomplished only a minor part of the process of estimating the reflectivity. The transition from nonstationary impulse response to reflectivity is much more difficult. Alternatively, if the reflectivity perspective is taken, then equation (28) is no longer sufficient because it does not allow for the attenuation of the seismic wavelet with traveltime. Thus for either case, equation (28) proves inadequate as a model for nonstationary deconvolution.

A nonstationary trace model

We now present a trace model that includes the source waveform and the nonstationary effects of dissipation as predicted by the constant-Q model though it does not explicitly model stratigraphic filtering. First, we consider the effect of constant Q and model it as

$$s_Q = \int_{-\infty}^{\infty} \int_{-\infty}^{\infty} \alpha_Q(\tau, f) r(\tau) e^{2\pi i f [\tau - \tau]} d\tau df \quad (29)$$

where $r(\tau)$ is explicitly the reflectivity and the constant-Q transfer function is

$$\alpha_Q(\tau, f) = e^{-\pi f \tau / Q + i H(\pi f \tau / Q)} \quad (30)$$

where H denotes the Hilbert transform over f at constant τ . Equation (29) can be understood as a nonstationary convolution by noting that the f integral can be written as

$$a_Q(\tau, t - \tau) = \int_{-\infty}^{\infty} \alpha_Q(\tau, f) e^{2\pi i f [t - \tau]} df \quad (31)$$

so that

$$s_Q = \int_{-\infty}^{\infty} a_Q(\tau, t - \tau) r(\tau) d\tau \quad (32)$$

which is a nonstationary convolution filter as defined by Margrave (1998). The forward Q nonstationary filter is defined by equations (30) and (31) and contains both the frequency dependent amplitude and phase effects of propagation in a dispersive medium.

As defined by equation (29), s_Q models dissipation for an impulsive source. For a more general source signature, we simply apply it with a stationary convolution and write our final nonstationary trace model as

$$\hat{s}(f) = \hat{w}(f) \int_{-\infty}^{\infty} \alpha_Q(\tau, f) r(\tau) e^{-2\pi i f \tau} d\tau \quad (33)$$

where \hat{w} and \hat{s} are the Fourier transforms of the source signature and the nonstationary seismic trace respectively. Equation (33) is our nonstationary trace model proposed as a replacement for the stationary convolution model of equation (28). We prefer to express it in the Fourier domain for simplicity.

Finally, since we apply the Gabor transform in our deconvolution method, the Gabor transform of $s(t)$, whose Fourier transform is given by equation (33), is desired. In Appendix B, we derive an asymptotic result for this as

$$V_g s(\tau, f) \approx \hat{w}(f) \alpha_Q(\tau, f) V_g r(\tau, f) \quad . \quad (34)$$

In words, the Gabor transform of our nonstationary trace is approximately equal to the product of the Fourier transform of the source signature, the constant Q transfer function, and the Gabor transform of the reflectivity. Since, for fixed τ , the Gabor transform is just a Fourier transform, this is a convolutional model in some local sense.

Figure 6 shows a pseudo-random reflectivity series and a nonstationary seismic trace constructed using a numerical implementation of equation (33) for a certain Q value and a minimum-phase source signature. Figure 7 is the magnitude of a Gabor transform of the nonstationary trace of Figure 6. The next sequence of figures illustrates the approximate decomposition of equation (34). Figure 8 is the magnitude of a Gabor transform of the reflectivity of Figure 6 computed using the same Gabor parameters as Figure 7. Figure 9 is the magnitude of the constant Q-transfer function as given by equation (30). The product of the functions of Figures 8 and 9 is shown in Figure 10. In comparison with Figure 7, Figure 10 is similar but lacks the restriction to the frequency band of the source signature. Figure 11 shows the magnitude of the source waveform as an invariant function of time. Finally the product of the functions of Figures 8, 9, and 11 completes the depiction of our spectral model of equation (34) and is shown in Figure 12. When this is compared with Figure 7, the correspondence is quite close but not exact. The slight variations are due to higher order terms that we have neglected in the approximate decomposition of equation (34).

A Gabor deconvolution algorithm

The broad picture is that we propose a method of deconvolution that constructs the Gabor transform of a nonstationary seismic trace and uses this information to estimate the Gabor transform of the reflectivity. From equation (34), this amounts to estimating both the source waveform and the Q transfer function and then dividing these out of the Gabor spectrum of the seismic trace. As with stationary deconvolution, this is an inherently nonunique *spectral factorization* problem that can only proceed by assuming certain properties about the three components of the right side of equation (34). From the outset, we will not attempt to measure phase and work only with the magnitude of equation (34). When an estimate of $|\hat{w}(f)| |\alpha_Q(\tau, f)|$ is available, a minimum-phase function will be calculated for it. We will also assume

that $|V_g r(\tau, f)|$ is a rapidly varying function in both variables as is seen in our example in Figure 3. In contrast, $|\hat{w}(f)|$ is assumed to be independent of τ and smooth in f while $|\alpha_Q(\tau, f)|$ is an exponential decay surface in both variables (see Figures 4 and 6). The assumptions we make about $|V_g r(\tau, f)|$ are similar to the *random reflectivity* assumption commonly made in stationary deconvolution theories; however, there is also a dependence upon the choice of Gaussian window. If the window is chosen to be excessively short in time then $|V_g r(\tau, f)|$ will be too smooth in frequency and vice-versa.

The simplest Gabor deconvolution algorithm estimates $|\hat{w}(f)||\alpha_Q(\tau, f)|$ by simply smoothing $|V_g s(\tau, f)|$ by convolving over (τ, f) with a 2-D boxcar. In many cases this is a surprisingly good estimate, although it is strongly dependent upon the size of the boxcar in both dimensions. There are many variations on this basic method such as using smoothers of different shapes (triangles or Gaussians for example). The basic drawback to the smoothing approach is that it will always result in a biased estimate of $|\hat{w}(f)||\alpha_Q(\tau, f)|$. To see this, suppose we have an extremely lucky case where $|V_g r(\tau, f)| \equiv 1$ so that $|V_g s(\tau, f)|$ is already equal to $|\hat{w}(f)||\alpha_Q(\tau, f)|$. Then, because the smoother will always alter the function to which it is applied, we obtain the wrong answer.

A more sophisticated approach might utilize an *a priori* guess of the values of Q say \tilde{Q} . Then, the smoothing bias can be reduced by forming $\overline{\overline{|\alpha_{-\tilde{Q}}(\tau, f)||V_g s(\tau, f)||\alpha_{\tilde{Q}}(\tau, f)|}}$, where the double overbar indicates a smoothing operation. In this expression, the Gabor transform of the seismic trace is multiplied by a positive exponential surface (i.e. $|\alpha_{-\tilde{Q}}(\tau, f)|$), the result is smoothed and then the exponential decay is restored with $|\alpha_{\tilde{Q}}(\tau, f)|$. This method has been explored by Schoepp and Margrave (1998), where it is shown to be more effective than simple smoothing provided that the estimated Q is close to the correct value.

Still more sophisticated is the possibility of estimating Q and $|\hat{w}(f)|$ by a least-squares fit of the model of equation (34) to $|V_g s(\tau, f)|$. This approach seems quite promising and is explored in Grossman et al. (2001).

Here we proceed with a description of the Gabor deconvolution procedure that works for any spectral factorization approach. Let $|V_g s(\tau, f)|_{sep}$ symbolize a suitably

smooth approximation to $|V_g s(\tau, f)|$, such that it is an acceptable estimation of $|\hat{w}(f)| |\alpha_Q(\tau, f)|$. Then, we invoke the minimum-phase assumption to obtain

$$\hat{w}(f) \alpha_Q(\tau, f) \approx |V_g s(\tau, f)|_{sep} e^{i\varphi(\tau, f)} \quad (35)$$

where the phase $\varphi(\tau, f)$ is given by the Hilbert transform expression

$$\varphi(\tau, f) = \int_{-\infty}^{\infty} \frac{\ln |V_g s(\tau, f')|_{sep}}{f - f'} df' \quad (36)$$

and is the *minimum-phase spectrum* corresponding to $|V_g s(\tau, f)|_{sep}$. Equation (35) is our estimate of the *propagating wavelet* that is the source signature as modified by attenuation and dispersion. Next we estimate the Gabor transform of the reflectivity by deconvolving the propagating wavelet from the Gabor transform of the seismic signal

$$V_g r(\tau, f)_{est} = \frac{|V_g s(\tau, f)|}{|V_g s(\tau, f)|_{sep}} e^{-i\varphi(\tau, f)} \quad (37)$$

and finally we perform the inverse Gabor Transform.

In any practical setting, it is almost always necessary to modify equation (37) to protect against division by very small numbers. Since $|V_g s(\tau, f)|_{sep}$ is modelled as a decaying exponential in both time and frequency, it will be especially small for large values of the product τf . This exponentially small signal will certainly be swamped by noise above some characteristic value of τf . Even in synthetic data there is a similar phenomenon brought about by the limited precision of floating point arithmetic. Both of these problems can be addressed by adding a small constant to the denominator of equation (37) as

$$V_g r(\tau, f)_{est} = \frac{|V_g s(\tau, f)|}{|V_g s(\tau, f)|_{sep} + \mu A_{max}} e^{-i\varphi(\tau, f)} \quad (38)$$

where μ is a small, dimensionless constant and A_{max} is the maximum of $|V_g s(\tau, f)|_{sep}$.

An interesting variant of the Gabor deconvolution algorithm can be done using the Burg spectral estimation (Claerbout 1976). Since the Burg method is often preferred on small data segments, it has obvious appeal when short temporal windows are desired. Our approach is to compute $V_g s(\tau, f)$ using the approximate discrete Gabor transform as discussed above and, simultaneously to compute a time-variant Burg

spectrum $V_B s(\tau, f)$. We compute the latter by calculating the Burg spectrum, in the usual fashion, for each Gaussian slice $s(\tau, t) = s(t)g(t - \tau)$. (Since the Burg spectrum has no phase, we don't bother with an absolute value sign for $V_B s(\tau, f)$. Also, we assume a Burg amplitude spectrum not a power spectrum.) The Burg time-variant spectrum is then used to design $|V_g s(\tau, f)|_{sep}$ and the entire process proceeds as before. Thus the only difference between our Burg approach and our Fourier approach is that the latter uses $|V_g s(\tau, f)|$ to design $|V_g s(\tau, f)|_{sep}$ while the former uses $V_B s(\tau, f)$. The advantage of the Burg approach is that $V_B s(\tau, f)$ is estimated as a very smooth function in f and usually needs additional smoothing in τ only.

Gabor deconvolution example

We now present an extended example of the Gabor deconvolution algorithm applied to a synthetic seismic trace. Figure 13 shows a pseudo-random reflectivity and a forward-Q filtered synthetic. In addition to the forward-Q operator, the synthetic also has been convolved with a stationary minimum-phase wavelet with a dominant frequency of 20 Hz. The synthetic signal shows both an overall decay of amplitude and a progressive spectral loss.

Figure 14 shows a Gabor spectrum of the synthetic signal of Figure 13. This was computed with $T = 0.1$ s and $\Delta\tau = 0.01$ s. The Gabor spectrum reveals that the signal contains the greatest power at early times and low frequencies. Next, Figure 15 is the result of smoothing the Gabor spectrum of Figure 14 by convolving it with a boxcar of dimensions 0.1 s by 20 Hz. This is taken to be an estimate of $|\hat{w}(f)| |\alpha_Q(\tau, f)|$. Then, Figure 16 is the deconvolved Gabor spectrum computed using equation (38). Since this is an estimate of the Gabor spectrum of the reflectivity, it is interesting to compare it to the correct result shown in Figure 17. The Gabor algorithm has achieved a very strong, broadband whitening but there are important differences in amplitudes between the deconvolution result and the answer. In Figure 18, the final deconvolved trace is shown in the time domain compared to the reflectivity. All of the major reflectors have been resolved but there are differences in amplitude. These amplitude differences are a consequence of the rather short temporal smoother that was used in this case. Such short smoothers tend to give strongly whitened results but also induce a kind of AGC (automatic gain correction).

We give other examples of Gabor deconvolution in other papers in this report. Henley and Margrave (2001) discuss a Promax implementation of Gabor deconvolution and demonstrate its performance on several test datasets. Iliescu and Margrave (2001) present a detailed comparison of processing a seismic line with Gabor deconvolution and compare it with Wiener spiking deconvolution. Grossman et al. (2001) show how to fit the nonstationary spectral model of equation (34) to the Gabor transform of a signal. Their method uses least squares and results in an estimate for $|\hat{w}(f)|$ and for Q and hence allows a deconvolution using constant-Q modified wavelet.

CONCLUSIONS

The Gabor transform decomposes a signal onto a time-frequency plane by windowing the signal with a sliding Gaussian and Fourier transforming. The Gaussian window used in the forward transform is called the analysis window. The inverse Gabor transform recreates the signal as a 2D integration over the time-frequency plane using a synthesis window. The theory of the Gabor transform can be developed for continuous or discrete window positions though the discrete theory is more difficult to develop precisely. The discrete Gabor transform can be more easily developed in an approximate way by using a special set of Gaussians whose width is related to their spacing in a controlled way. The discrete Gabor transform is lossy (the result of a forward and inverse transform does not exactly replicate the signal) but the error is easily controlled to lie below any given tolerance.

Gabor filtering is implemented by multiplying the Gabor transform of a signal by a time-frequency filter specification. Two end-member cases of Gabor filters were identified and shown to be equivalent to normal or adjoint pseudodifferential operators.

Gabor deconvolution can be developed based on a nonstationary extension of the common convolutional model of a seismic trace. Using Gabor theory, this nonstationary convolutional model implies that the Gabor transform of a seismic trace can be written as the Fourier spectrum of the source signature, times a forward-Q filter, times the Gabor transform of the reflectivity. Gabor deconvolution requires the spectral factorization of the Gabor transform of the signal into two terms, one representing the Gabor transform of the reflectivity and the other representing the source signature times the forward-Q filter. This factorization can be carried out on the magnitude of the Gabor transform of the signal with the phase terms being calculated by a minimum-phase condition. Tests on synthetic data shows that the algorithm produces an excellent reflectivity estimate from a nonstationary synthetic.

FUTURE RESEARCH DIRECTIONS

The approximate Gabor transform algorithm used here will be compared with the exact, discrete Gabor transform. This should allow a more efficient process. The impact of the Gabor transform parameters (window width and increment) needs to be assessed. Other window shapes might be more appropriate to model nonstationary minimum-phase processes. The ability of this approach to model and remove the nonstationary multiple train needs investigation. The deconvolution process can almost certainly be improved by the incorporation of more information about the reflectivity. The performance of this approach needs to be compared with the pseudodifferential operator approach of Schoepp and Margrave (1998). The Q-estimation algorithm of Grossman et al. (2001) is very promising and needs evolution.

ACKNOWLEDGEMENTS

We benefited from a series of valuable discussions with Jeff Grossman, Victor Iliescu, Kris Vasudevan, and Rita Aggarwala. These discussions occurred in a weekly seminar on Gabor Analysis, led by the POTSI project, which the authors have

participated in over the past spring and summer sessions at the University of Calgary. (POTSI, or *Pseudodifferential Operator Theory in Seismic Imaging*, is a collaborative research project between the University of Calgary departments of Mathematics and Geophysics (supported by MITACS), Imperial Oil, CREWES, and NSERC.)

We gratefully acknowledge financial support from NSERC, MITACS, and CREWES.

REFERENCES

- Bastiaans, M.J., 1980, Gabor's expansion of a signal into Gaussian elementary signals: Proceedings of the IEEE, **68**, 538-539.
- Brigham, E.O., 1974, The Fast Fourier Transform: Prentice-Hall, ISBN 0-13-307496-X.
- Claerbout, J., 1976, Fundamentals of Geophysical Data Processing:
- Feichtinger, H.G. and Strohmer, T., 1998, Gabor analysis and algorithms: Theory and applications: Birkhauser, ISBN 0-8176-3959-4.
- Futterman, W.I., 1962, Dispersive body waves: J. Geophys. Res., **67**, 5279-91.
- Gabor, D., 1946, Theory of communication: J. IEEE (London), **93(III)**, 429-457.
- Grossman, J.P., Margrave, G.F., Lamoureux, M.P., and Aggarwala, R., 2001, Constant-Q wavelet estimation via a nonstationary Gabor spectral model: CREWES Annual Research Report, **13**.
- Henley, D. and Margrave, G.F., 2001, A ProMAX implementation of nonstationary deconvolution: CREWES Annual Research Report, **13**.
- Kjartansson, E., 1979, Constant Q-wave propagation and attenuation: Journal of Geophysical Research, **84**, 4737-4748.
- Iliescu, V. and Margrave, G.F., 2001, Gabor deconvolution applied to a Blackfoot dataset: CREWES Annual Research Report, **13**.
- Margrave, G.F., 1998, Theory of nonstationary linear filtering in the Fourier domain with application to time-variant filtering: Geophysics, **63**, 244-259.
- Mertins, A., 1999, Signal Analysis: John Wiley and Sons, ISBN 0-471-98626-7.
- O'Doherty, R.F. and Anstey, N.A., 1971, Reflections on amplitudes: Geophys. Prosp., **19**, 430-58.
- Peacock, K.L. and Treitel, S., 1969, Predictive deconvolution: Theory and practice: Geophysics, **34**, 155-169.
- Robinson, E.A. and Treitel, S., 1967, Principles of digital Wiener filtering: Geophys. Prosp., **15**, 311-333.
- Schoepp, A.R. and Margrave, G.F., 1998, Improving seismic resolution with nonstationary deconvolution: 68th Annual SEG meeting, New Orleans, La.

APPENDIX A: GAUSSIAN SUMMATION CONDITION

Here we derive an analytic formula for the sum of a sequence of Gaussians. Specifically, let the Gaussians be given by

$$g(t - k\Delta\tau) = \frac{\Delta\tau}{T\sqrt{\pi}} e^{-[t-k\Delta\tau]^2 T^{-2}} \quad (\text{A-1})$$

and we desire an expression for $\sum_k g(t - k\Delta\tau)$. This sum can be written as the convolution of an unshifted Gaussian with a Dirac comb

$$h(t) \equiv \sum_{k \in \mathbb{Z}} g(t - k\Delta\tau) = (g \bullet c)(t) \quad (\text{A-2})$$

where $g(t) = T^{-1}\pi^{-1/2} \Delta\tau e^{-[t/T]^2}$ and $c(t) = \sum_k \delta(t - k\Delta\tau)$. Both of these functions have known Fourier transforms that can be found in Brigham (1974)

$$\hat{g}(f) = \Delta\tau e^{-[\pi f T]^2} \quad (\text{A-3})$$

and

$$\hat{c}(f) = \frac{1}{\Delta\tau} \sum_k \delta\left(f - \frac{k}{\Delta\tau}\right). \quad (\text{A-4})$$

Therefore, by the convolution theorem

$$h = F^{-1}(\hat{g}\hat{c}) = F^{-1}\left(\cdots \delta\left(f + \frac{1}{\Delta\tau}\right)e^{-[\pi f T]^2} + \delta(f)e^{-[\pi f T]^2} + \delta\left(f - \frac{1}{\Delta\tau}\right)e^{-[\pi f T]^2} + \cdots\right) \quad (\text{A-5})$$

where F^{-1} is the inverse Fourier transform. Using the delta function to evaluate the transforms shows the central term is unity while the two neighbouring terms are

$$\begin{aligned} F^{-1}\left(\delta\left(f + \frac{1}{\Delta\tau}\right)e^{-[\pi f T]^2} + \delta\left(f - \frac{1}{\Delta\tau}\right)e^{-[\pi f T]^2}\right) &= e^{-[\pi T/\Delta\tau]^2} [e^{2\pi i t/\Delta\tau} + e^{-2\pi i t/\Delta\tau}] \\ &= 2\cos(2\pi t/\Delta\tau)e^{-[\pi T/\Delta\tau]^2} \end{aligned} \quad (\text{A-6})$$

Thus we conclude

$$h(t) = 1 + 2\cos(2\pi t/\Delta\tau)e^{-[\pi T/\Delta\tau]^2} + \dots \quad (\text{A-7})$$

Furthermore, because the higher order terms are integrated against delta functions with higher frequency arguments (larger values of $k/\Delta\tau$) they are exponentially smaller with each value of k .

APPENDIX B: JUSTIFICATION OF THE TIME-VARIANT SPECTRAL MODEL USING GABOR TRANSFORMS.

Let $r(t)$ be a (random) reflectivity, $w(t)$ a wavelet, and $\alpha(t, f)$ the time-frequency symbol of a constant Q operator. Specifically for the latter

$$\alpha(t, f) = e^{-\pi f t/Q - iH(\pi f t/Q)} \quad (\text{B-1})$$

where H denotes the Hilbert transform. An assumption is that $\hat{w}(f)$ (the Fourier transform of the wavelet) is smooth. Note that $\alpha(t, f)$ is also reasonably smooth.

Then a nonstationary synthetic can be constructed by a nonstationary convolution of the Q operator and the reflectivity and then a stationary convolution with the wavelet. Letting $s(t)$ denote the nonstationary synthetic trace, then using the mixed domain form of nonstationary convolution gives

$$\hat{s}(f) = \hat{w}(f) \int_{-\infty}^{\infty} \alpha(t, f) r(t) e^{-2\pi ift} dt \quad (\text{B-2})$$

where the hat denotes the Fourier transform. Thus

$$\begin{aligned} s(t) &= \int_{-\infty}^{\infty} \hat{w}(f) \left[\int_{-\infty}^{\infty} \alpha(u, f) r(u) e^{-2\pi ifu} du \right] e^{2\pi ift} df \\ &= \iint \hat{w}(f) \alpha(u, f) r(u) e^{2\pi if[t-u]} df du \end{aligned} \quad (\text{B-3})$$

This may seem a bit lacking in justification but is, in fact, quite well established. We now want to show that a time-frequency decomposition of $s(t)$, call it $Ts(\tau, v)$, has the approximate factorization: $Ts(\tau, v) \sim \hat{w}(v) \alpha(\tau, v) Tr(\tau, v)$. Here $Tr(\tau, v)$ is the time-frequency decomposition of the reflectivity. This will be demonstrated using Gabor spectra as the time-frequency decomposition.

Now, the Gabor transform of $s(t)$ is defined as

$$V_g s(\tau, v) = \int_{-\infty}^{\infty} s(t) g(t - \tau) e^{-2\pi i v t} dt \quad (\text{B-4})$$

where $g(t)$ is the Gabor analysis window (usually a Gaussian). Substituting (B-3) into (B-4) gives

$$V_g s(\tau, v) = \int_{-\infty}^{\infty} \left[\iint \hat{w}(f) \alpha(u, f) r(u) e^{2\pi if[t-u]} df du \right] g(t - \tau) e^{-2\pi i v t} dt. \quad (\text{B-5})$$

Consider the t integral in equation (B-5)

$$I = \int g(t - \tau) e^{-2\pi i t [v - f]} dt. \quad (\text{B-6})$$

Let $t' = t - \tau$ and so

$$I = \int g(t') e^{-2\pi i [t' + \tau] [v - f]} dt' = e^{-2\pi i \tau [v - f]} \hat{g}(v - f) \quad (\text{B-7})$$

So that equation (B-5) becomes

$$V_g s(\tau, v) = \iint \hat{w}(f) \alpha(u, f) r(u) e^{-2\pi ifu} e^{-2\pi i \tau [v - f]} \hat{g}(v - f) df du \quad (\text{B-8})$$

Now, let $f' = v - f$ so that

$$V_g s(\tau, v) = \iint \hat{w}(v - f') \alpha(u, v - f') r(u) e^{-2\pi i [v - f'] u} e^{-2\pi i \tau f'} \hat{g}(f') df' du \quad (\text{B-9})$$

Then, using Taylor series

$$\begin{aligned} V_g s(\tau, v) &= \iint \left[\hat{w}(v) - \frac{\partial \hat{w}}{\partial v}(v) f' + \dots \right] \\ &\quad \left[\alpha(u, v) - \frac{\partial \alpha}{\partial v}(u, v) f' + \dots \right] r(u) e^{-2\pi i [v - f'] u} e^{-2\pi i \tau f'} \hat{g}(f') df' du \end{aligned} \quad (\text{B-10})$$

or

$$V_g s(\tau, v) = \hat{w}(v) \int \alpha(u, v) r(u) e^{-2\pi i v u} \left[\int e^{2\pi i [u - \tau] f'} \hat{g}(f') df' \right] du + \dots \quad (\text{B-11})$$

or

$$V_g s(\tau, v) = \hat{w}(v) \int \alpha(u, v) r(u) g(u - \tau) e^{-2\pi i v u} du + \dots \quad (\text{B-12})$$

let $u' = \tau - u$

$$V_g s(\tau, v) = \hat{w}(v) \int \alpha(\tau - u', v) r(\tau - u') g(-u') e^{-2\pi i v [\tau - u']} du' + \dots \quad (\text{B-13})$$

expand $\alpha(\tau - u', v)$ in a Taylor series

$$V_g s(\tau, v) = \hat{w}(v) \alpha(\tau, v) \int r(\tau - u') g(-u') e^{-2\pi i v [\tau - u']} du' + \dots \quad (\text{B-14})$$

now, back to $u = \tau - u'$

$$V_g s(\tau, v) = \hat{w}(v) \alpha(\tau, v) \int r(u) g(u - \tau) e^{-2\pi i v u} du + \dots \quad (\text{B-15})$$

or

$$V_g s(\tau, v) = \hat{w}(v) \alpha(\tau, v) V_g r(\tau, v) + \dots \quad (\text{B-16})$$

These last several manipulations seem almost circular but they amount to a justification that $\alpha(u, v)$ can be pulled out of the integral in equation (B-12) where it becomes $\alpha(\tau, v)$. This analysis shows the leading-order behaviour fits the nonstationary model but so far provides no estimate of the next asymptotic term.

FIGURES

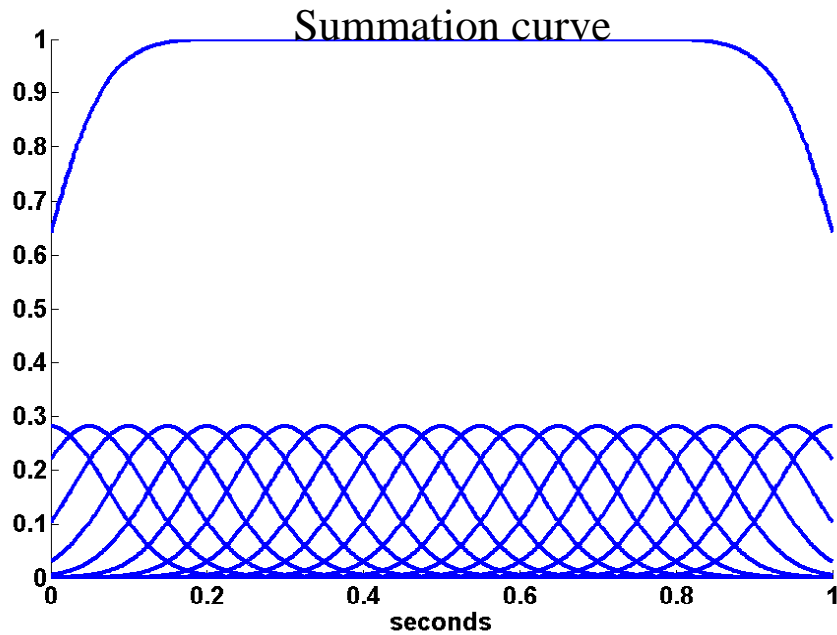


FIG. 1. The summation of a set of Gaussian windows is illustrated. The window half-width is 0.1 seconds and the window increment is 0.05 seconds.

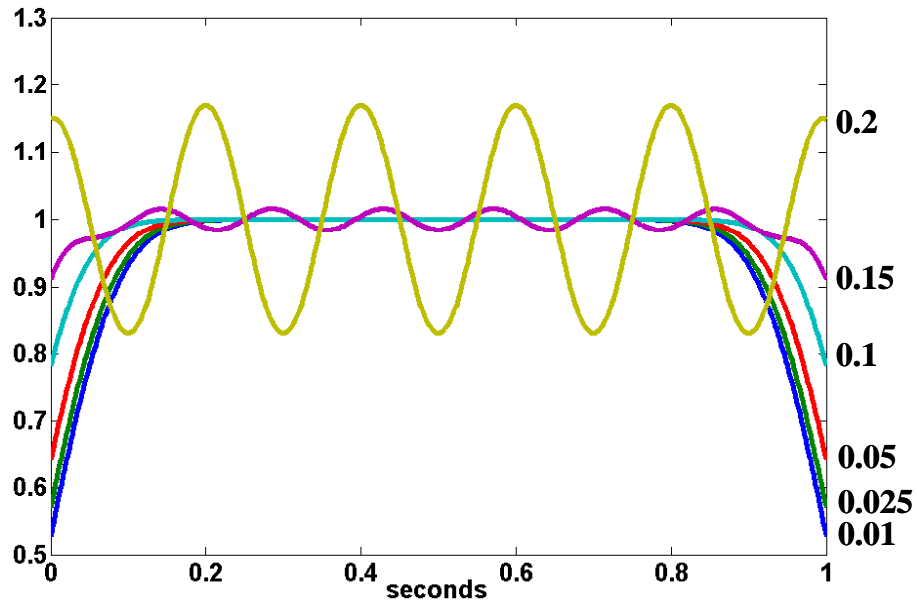


FIG. 2. The summation curves for a suite of different Gaussian summations are shown for a window half-width of .1 seconds. Each summation curve is labelled with its window increment. When the window increment significantly exceeds the half-width, then the summation is no longer close to unity.

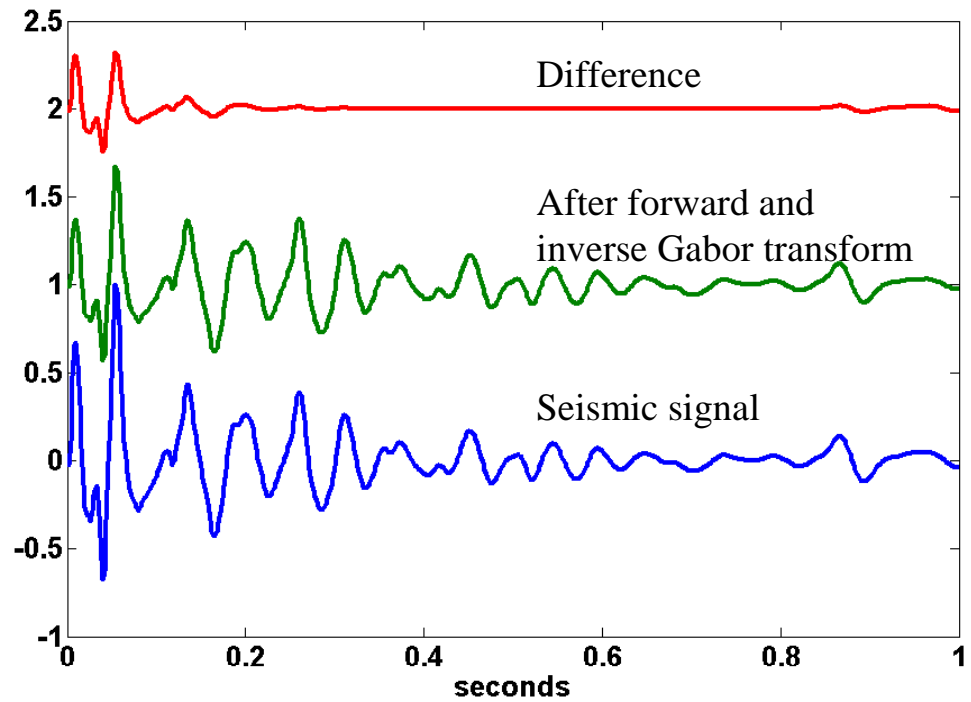


FIG. 3. The result of a forward and inverse Gabor transform using the approximate algorithm (equations (18) and (21)) is compared with the original signal. The largest differences are found at the ends of the signal where the Gaussian summation has the largest departure from unity.

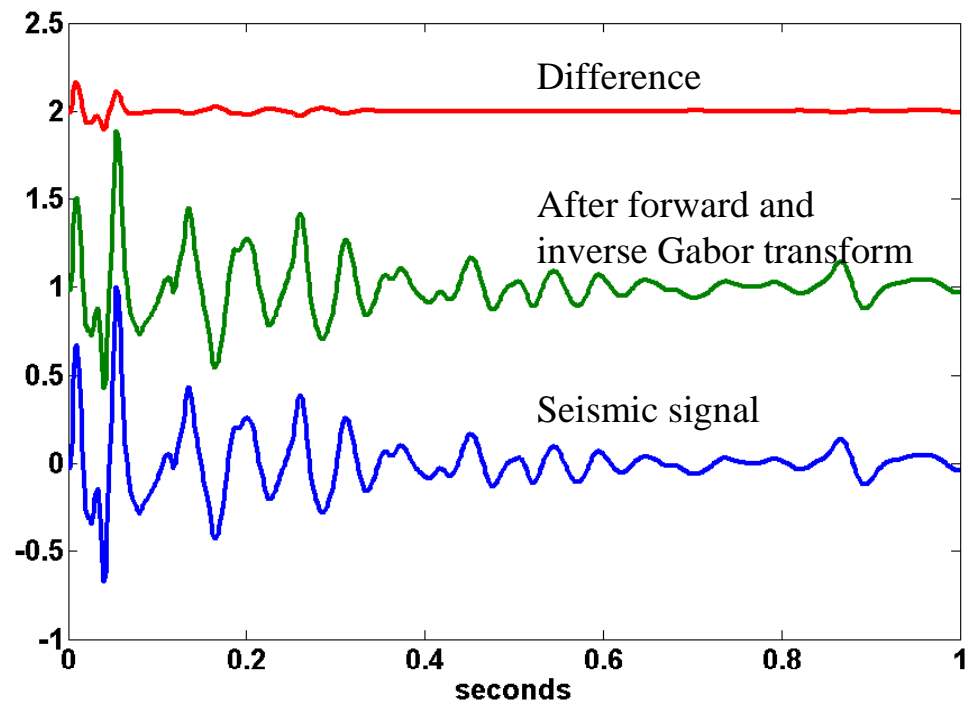


FIG. 4. The comparison of Figure 3 is repeated but the forward Gabor transform uses the normalized expression of equation (18a) instead of (18). The end effects are clearly reduced.

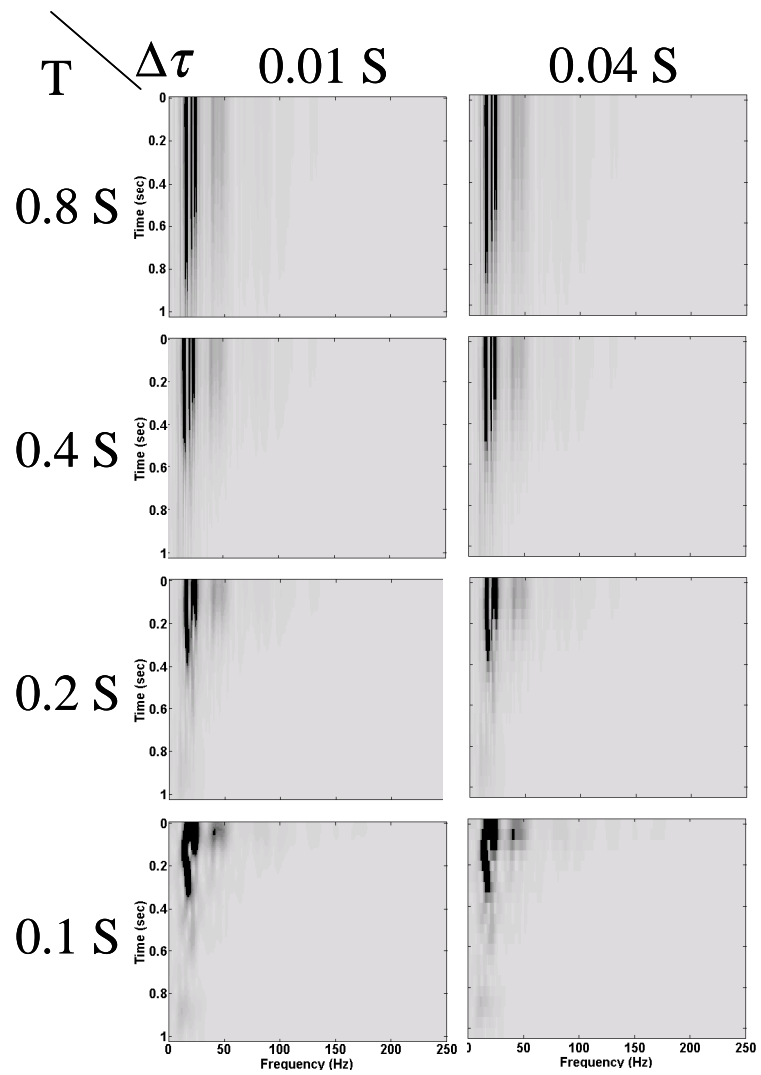


FIG. 5. The Gabor transform of the signal of Figure 3 is shown for a variety of window widths and increments. The highest frequency resolution and lowest temporal resolution occurs at the left while the highest temporal resolution and lowest frequency resolution is on the right.

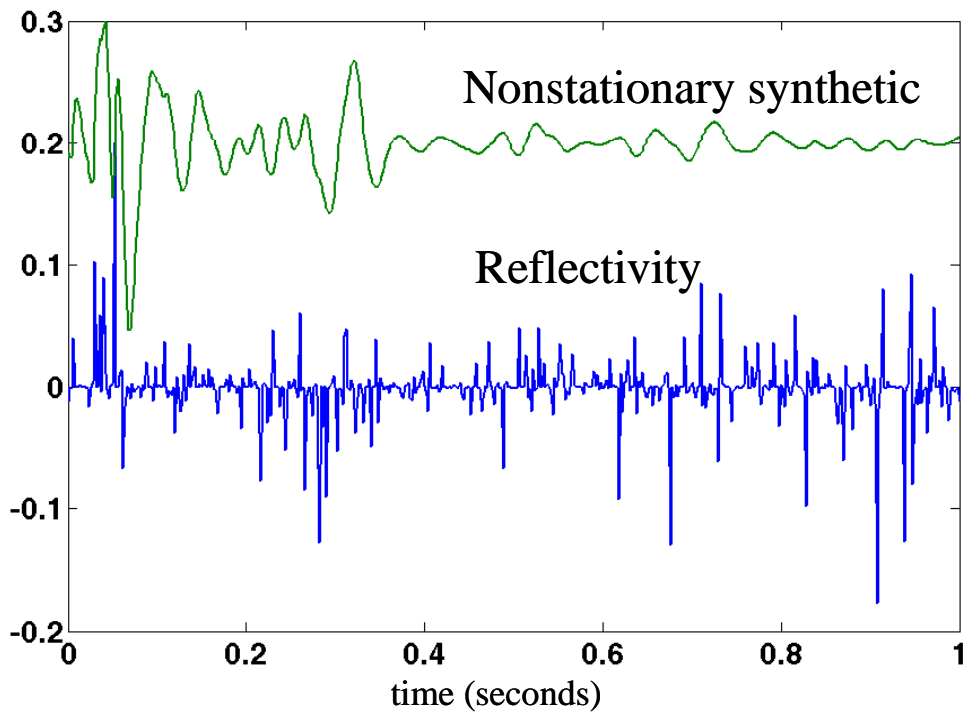


FIG. 6. A pseudo-random reflectivity (bottom) and a nonstationary seismic trace (top).

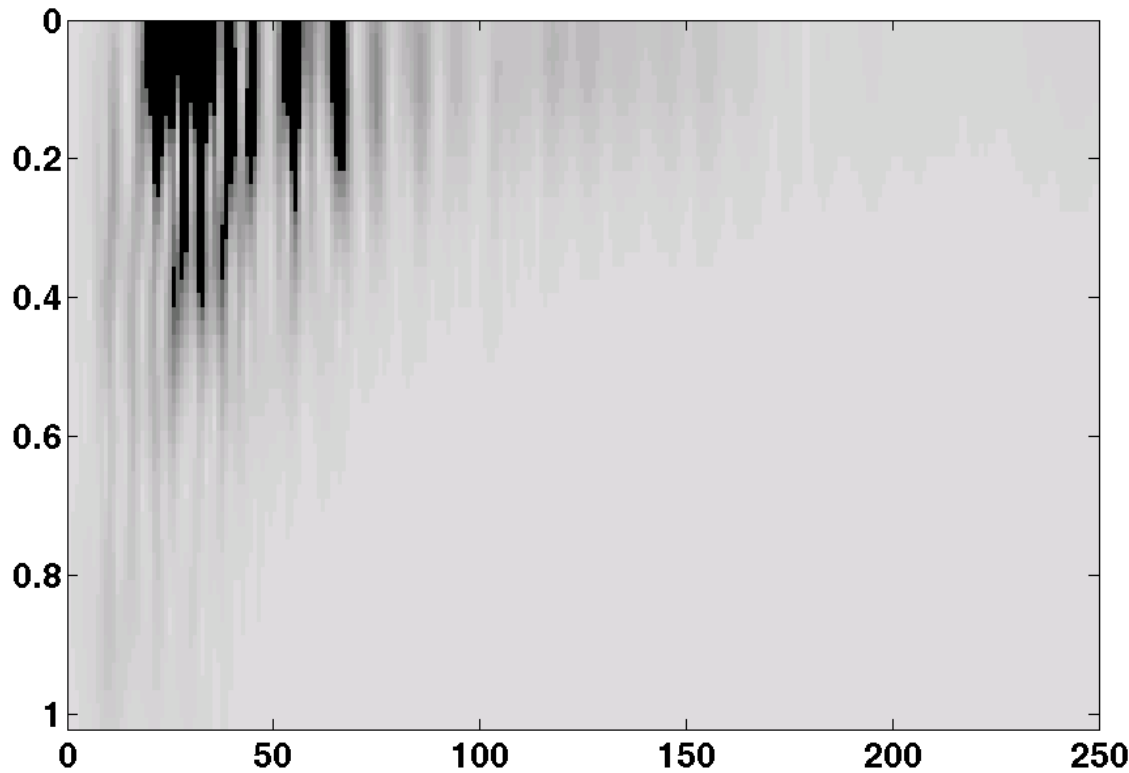


FIG. 7. The magnitude of the Gabor transform of the nonstationary time series of Figure 1.

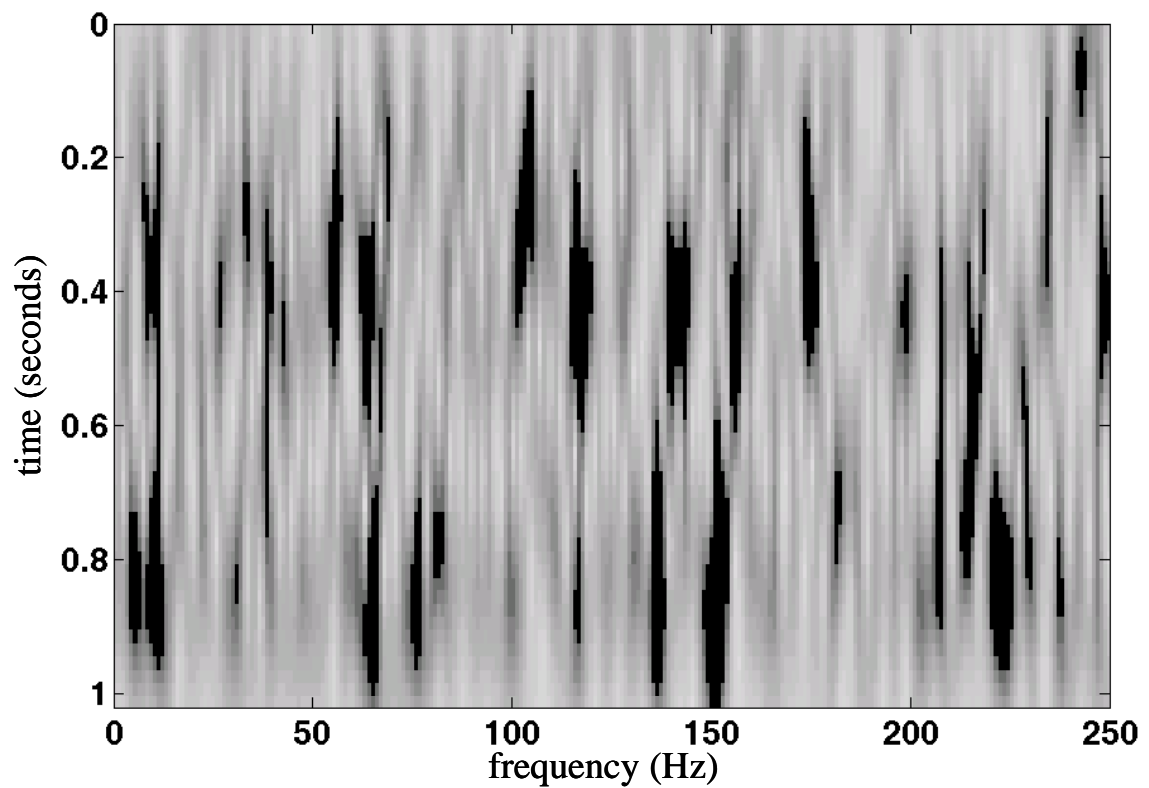


FIG. 8. The magnitude of the Gabor transform of the reflectivity of Figure 7.

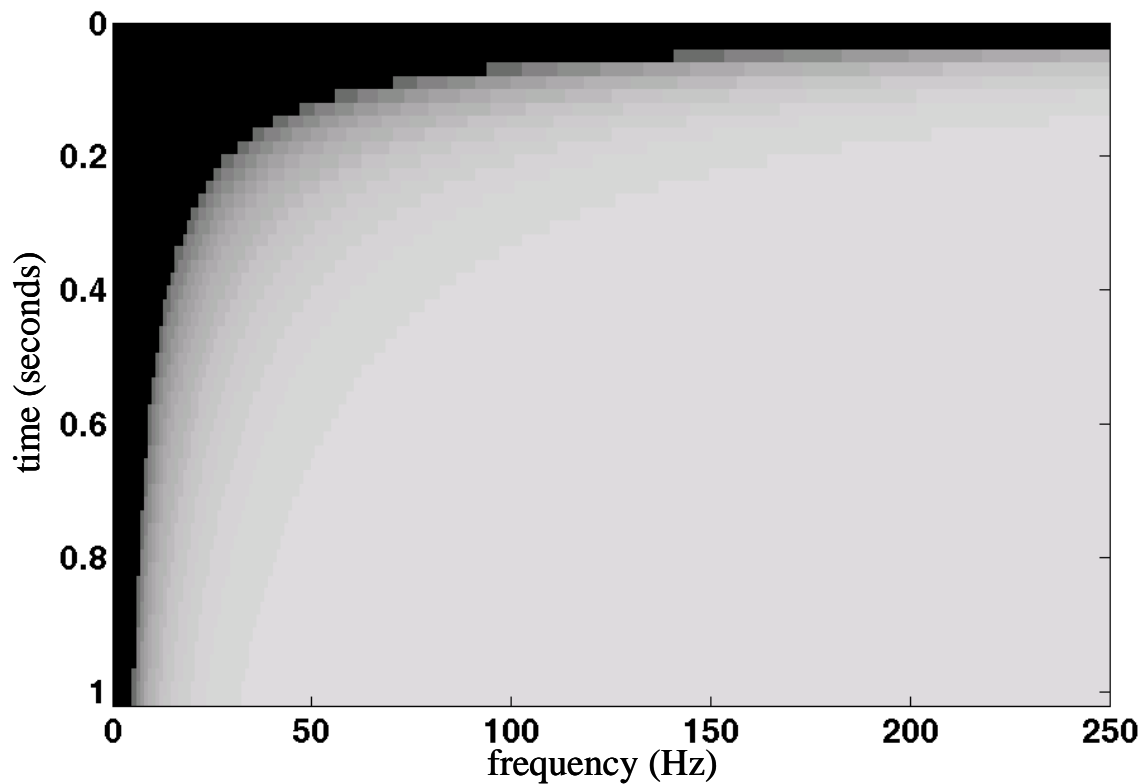


FIG. 9. The function $e^{-\pi f t / Q}$ representing the forward-Q operator.

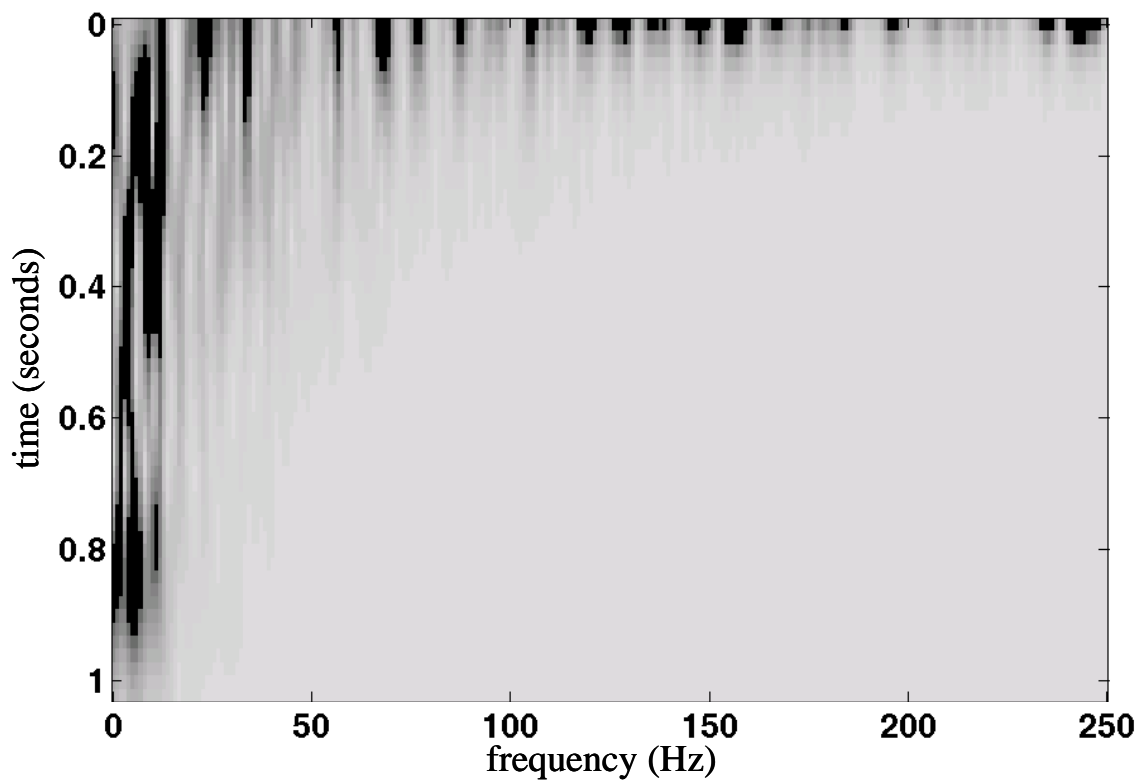


FIG. 10. The pointwise product of the Gabor transform of the reflectivity (Figure 7) and the forward-Q operator (Figure 8).

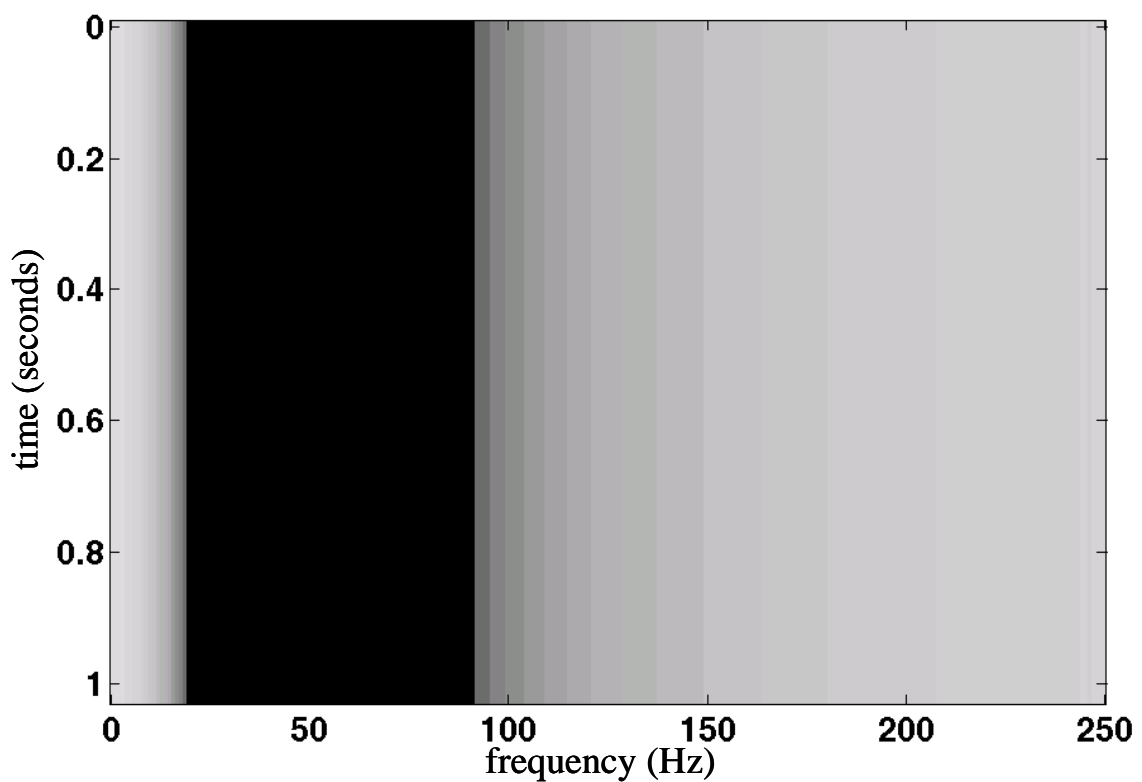


FIG. 11. A stationary wavelet represented on a time-frequency plane.

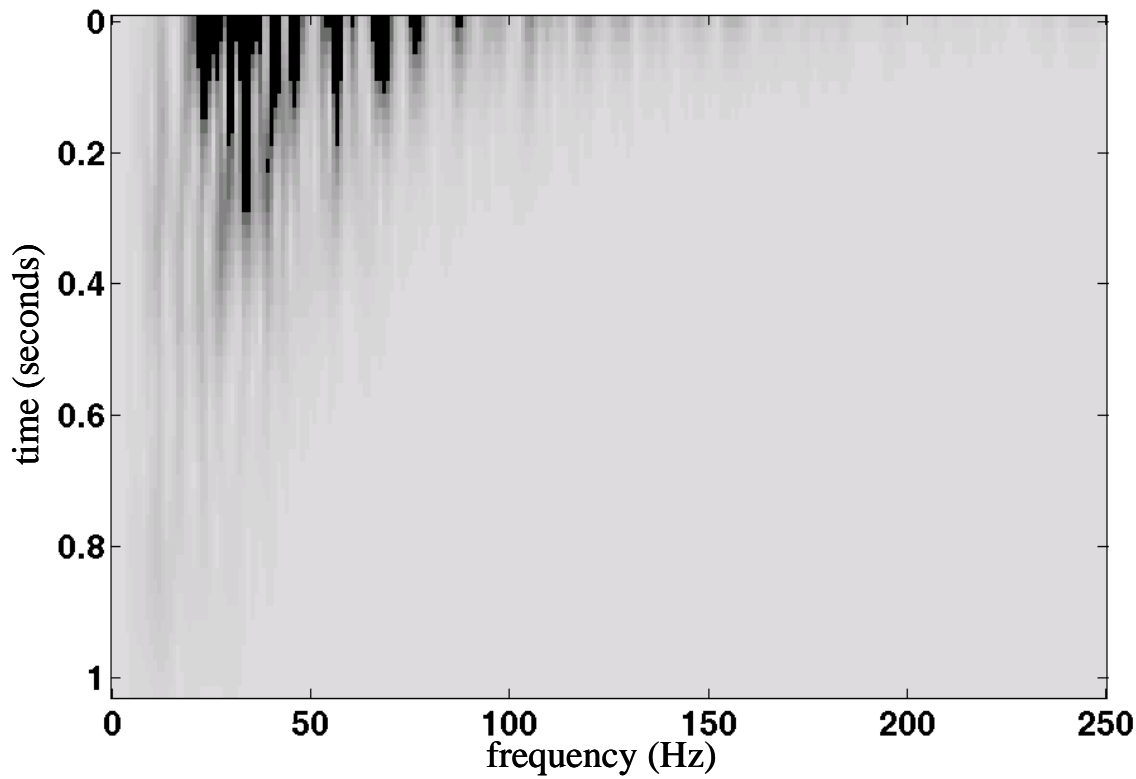


FIG. 12. The pointwise product of the Gabor transform of the reflectivity (Figure 8) with the forward-Q operator (Figure 9) and with the wavelet (Figure 10). Comparison with Figure 7 shows that this is a good representation of the Gabor spectrum of the nonstationary synthetic.

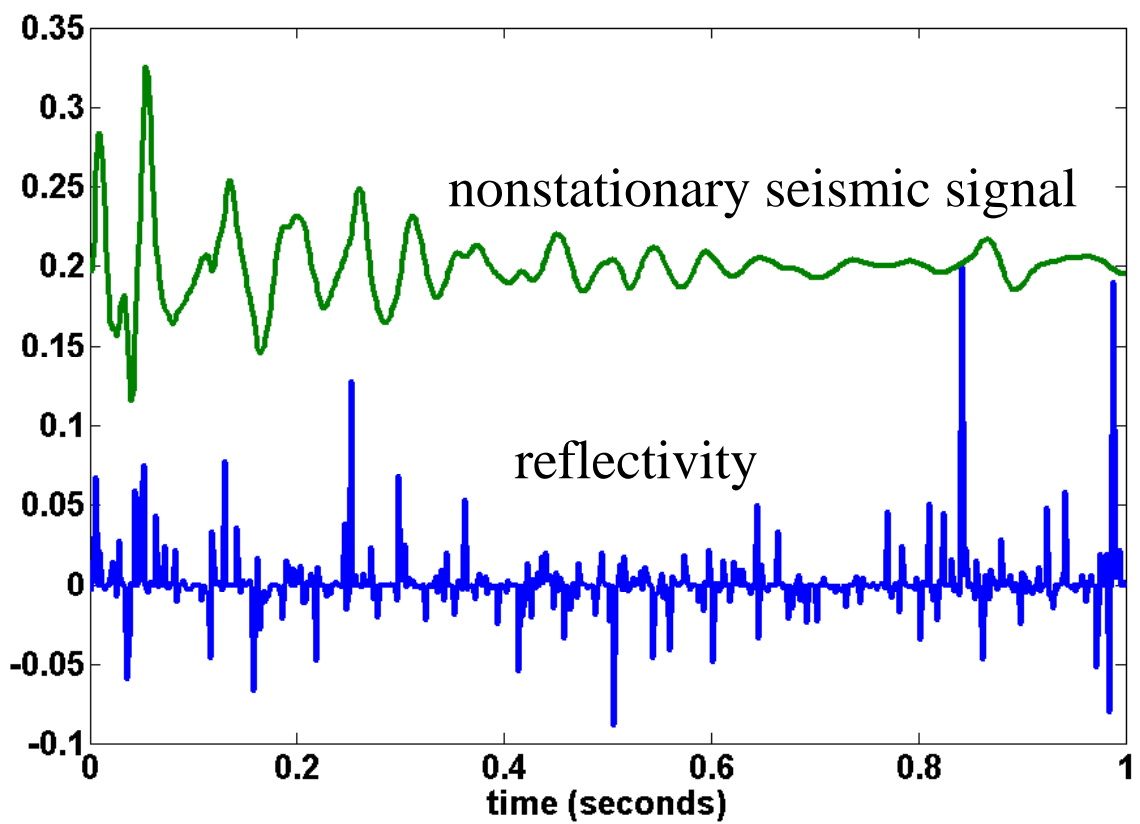


FIG 13. A pseudo-random reflectivity is show (bottom) and a nonstationary seismic signal created from the reflectivity (top). The nonstationary signal has a minimum phase source signature and a minimum-phase forward-Q filter applied.

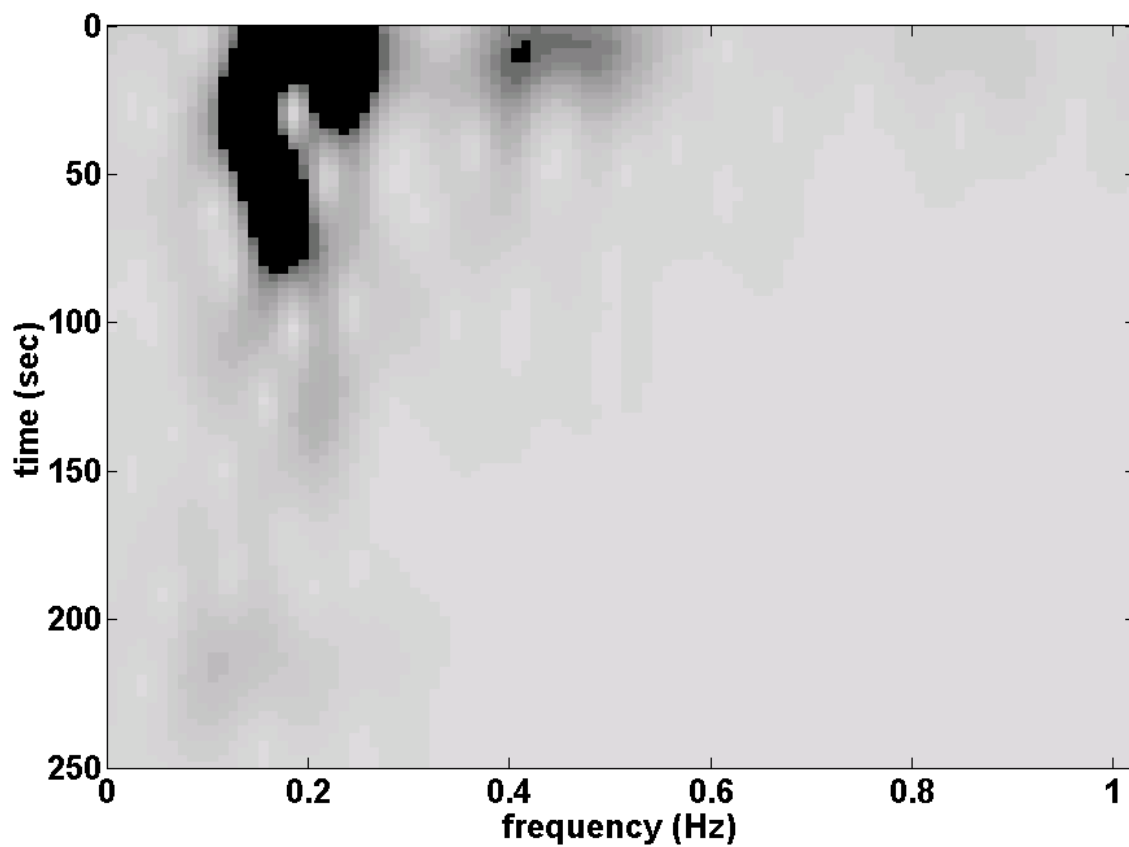


FIG. 14. The magnitude of the Gabor transform of the nonstationary seismic signal of Figure 13 is shown. The Gaussian half-width was 0.1s and the increment between Gaussian windows was 0.01s.

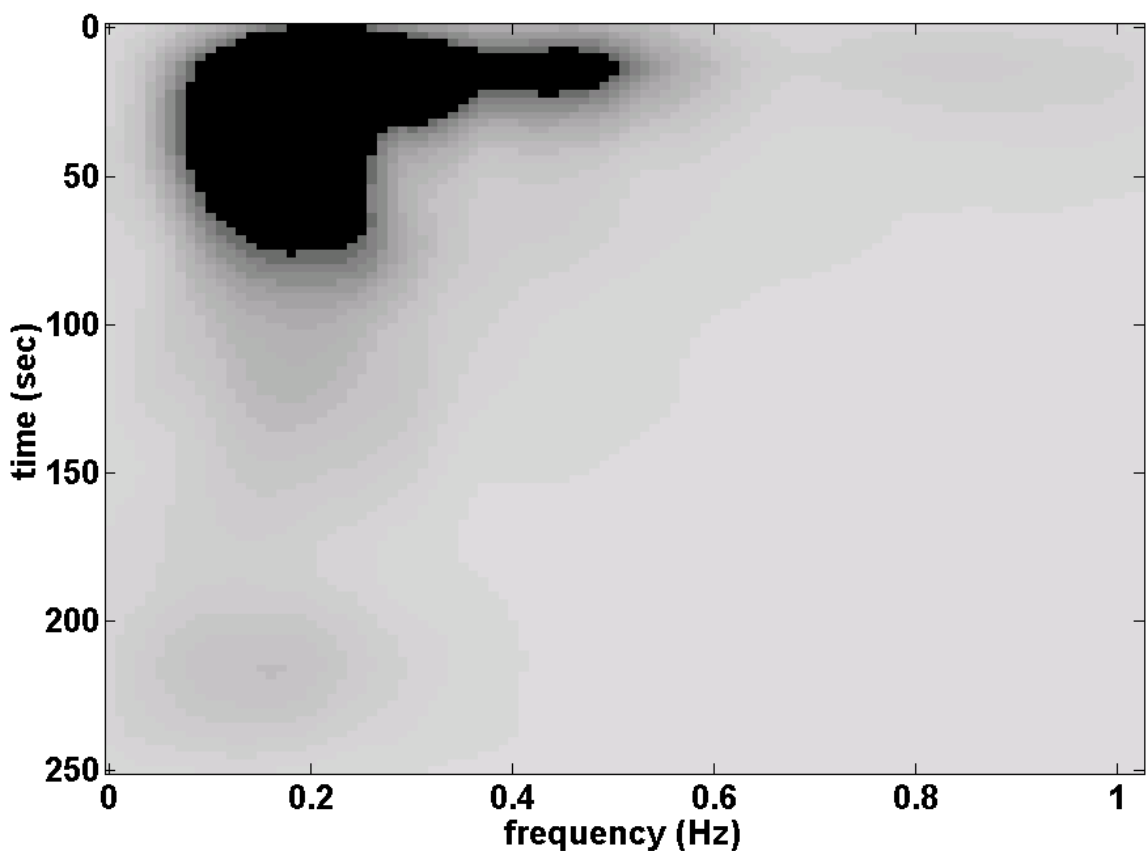


FIG. 15. The magnitude of the Gabor transform of Figure 14 after smoothing by convolution with a 2-D boxcar of dimensions 0.1s by 20Hz.

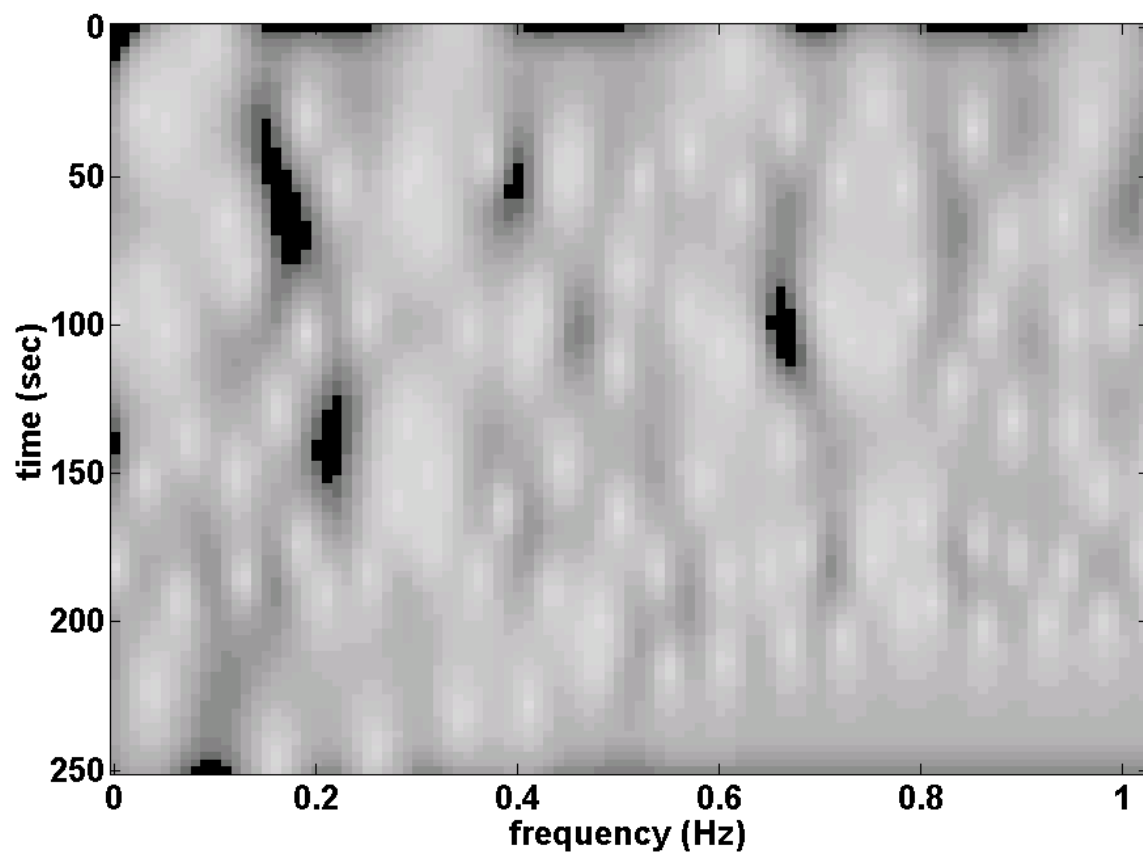


FIG 16. The result of dividing the Gabor transform of Figure 14 by that of Figure 15 using the procedure described in the text. This is an estimate of the Gabor transform of the reflectivity.

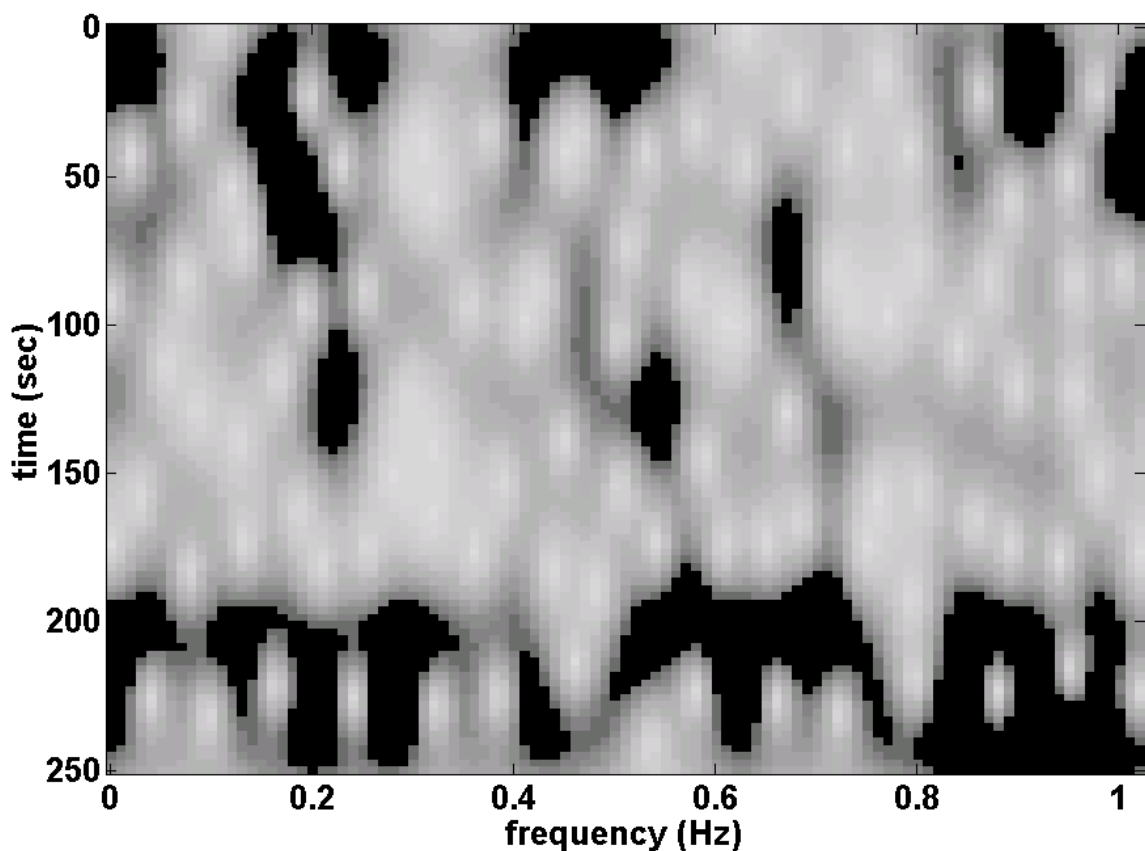


FIG. 17. This is the magnitude of the Gabor transform of the reflectivity signal shown in Figure 13. It was computed with the same Gabor parameters as Figure 14. Figure 16 is an estimate of this transform produced by Gabor deconvolution.

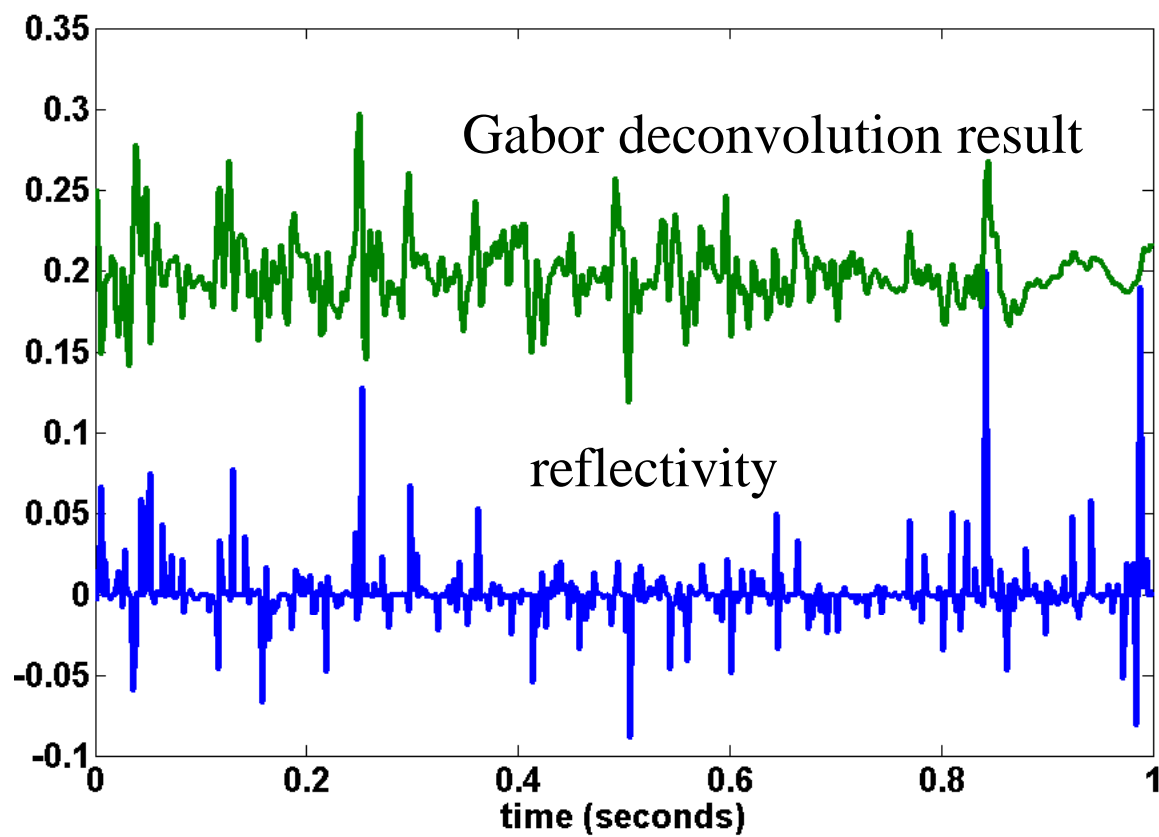


FIG 18. On top is a Gabor deconvolution of the nonstationary seismic signal of Figure 13. It is the inverse Gabor transform of the Gabor spectrum of Figure 16. In comparison with the true reflectivity, there is a general correspondence of major peaks.